

Efficient Hybrid CNN-GNN Architecture for Monocular Depth Estimation

Ishan Narayan

IMCS Lab, CSIR-CSIO

Chandigarh 160030, India

ishan.csio21a@acsir.res.in

Abstract

We present **GraphDepth**, a monocular depth estimation architecture that synergistically integrates Graph Neural Networks (GNNs) within a convolutional encoder-decoder framework. Our approach embeds efficient GraphSAGE layers at multiple scales of a ResNet-101 U-Net backbone, enabling explicit modeling of long-range spatial relationships that lie beyond the receptive field of local convolutions. Key technical contributions include: (1) batch-parallelized graph construction with configurable k -NN and grid-based adjacency for scalable training; (2) multi-scale GraphSAGE integration at bottleneck and decoder stages (1/32, 1/16, 1/8 resolution) to propagate global context throughout the feature hierarchy; (3) channel-attention gated skip connections that adaptively weight encoder features before fusion; and (4) heteroscedastic uncertainty estimation via a dedicated aleatoric uncertainty head, enabling confidence-aware loss weighting during optimization. Unlike transformer-based hybrids, which suffer from quadratic complexity in sequence length, GraphDepth scales linearly with spatial resolution while achieving comparable global receptive fields through iterative message passing. Experiments on NYU Depth V2, WHU Aerial, ETH3D, and Mid-Air benchmarks demonstrate competitive accuracy—within 4.6% of state-of-the-art transformers on indoor scenes—with substantially lower computational cost (25 FPS vs. 9 FPS, 3.8 GB vs. 8.8 GB VRAM). GraphDepth achieves the best reported result on WHU Aerial (RMSE 8.24 m) and exhibits superior zero-shot cross-domain transfer to the Mid-Air synthetic aerial dataset, validating the generalization power of explicit relational reasoning for depth estimation.

Keywords: monocular depth estimation, graph neural networks, GraphSAGE, U-Net, encoder-decoder, uncertainty estimation.

1. Introduction

Monocular depth estimation (MDE) is a fundamental computer vision task with critical applications in autonomous driving, augmented reality, and robotic navigation [1]. Despite remarkable progress, the field still grapples with a core tension: *local feature extraction* versus *global context modeling*.

CNN limitations. Convolutional Neural Networks (CNNs) have long dominated MDE owing to their inductive biases for spatial locality and computational efficiency. However, their bounded receptive fields constrain the capture of long-range geometric dependencies, particularly in scenes containing large uniform regions, distant objects, or complex occlusion patterns.

Transformer limitations. Vision Transformers (ViTs) address this by exploiting self-attention over full spatial sequences [6, 7]. Although they achieve state-of-the-art MDE accuracy, their self-attention complexity is quadratic in sequence length—prohibitively expensive at high resolutions required for real-world deployment. Recent studies further reveal that transformers may underweight fine-grained local detail that CNNs naturally preserve.

GNN opportunity. Graph Neural Networks (GNNs) are an underexplored alternative that avoids both pitfalls. By representing image features as graph nodes and spatial relationships as edges, GNNs perform message passing with sub-quadratic complexity while explicitly encoding geometric structure. GraphSAGE [9] in particular offers inductive capability and flexible neighborhood aggregation that aligns naturally with hierarchical encoder-decoder processing. However, prior work applying GNNs to dense prediction tasks has typically processed extracted features in isolation rather than embedding GNNs directly within the CNN feature hierarchy, leaving their potential underutilized [8].

Contributions. We propose **GraphDepth**, which addresses three critical gaps:

1. **Scalable batch graph construction.** We implement batch-parallelized k -NN and grid-based adja-

gency that avoids Python-level loops and supports mixed-precision training.

- 2. Multi-scale GNN reasoning.** GraphSAGE layers are embedded at the bottleneck and two decoder stages, propagating relational context across the feature pyramid.
- 3. Uncertainty-aware training.** A heteroscedastic uncertainty head learns per-pixel confidence maps that modulate the training loss, reducing overconfident errors under domain shift.

We provide thorough evaluation on indoor, aerial, and synthetic benchmarks, including a zero-shot cross-domain transfer experiment, and demonstrate that our hybrid design achieves favorable accuracy-efficiency trade-offs compared with both CNN and transformer baselines.

2. Related Work

CNN-based depth estimation. Eigen et al. [1] introduced the multi-scale CNN paradigm for MDE. Encoder-decoder architectures with skip connections [2, 14] improved structural fidelity. BTS [4] further refined this with local planar guidance modules that exploit multi-scale plane estimates. AdaBins [5] reframed depth regression as adaptive histogram binning, achieving strong performance on NYU Depth V2. These works share an inherent limitation: their receptive fields are bounded by kernel sizes and pooling strides, making global context aggregation costly.

Transformer-based depth estimation. DPT [6] repurposed a ViT backbone with a convolutional decode head and demonstrated that long-range self-attention yields substantial gains over pure CNNs. DepthFormer [7] further combined a Swin-based encoder with a cross-attention decoder to exploit multi-scale global correlations. Despite their accuracy, transformer architectures carry prohibitive memory and compute costs at high resolution and tend to lose fine-grained local texture detail.

Hybrid architectures. Several works have explored combining CNN encoders with attention-augmented decoders. However, these hybrids typically introduce dense attention operations that retain quadratic scaling, or they apply attention only at a single scale, limiting context propagation. Our method is architecturally distinct: we embed GraphSAGE *inside* the feature hierarchy at multiple scales, coupling local convolutional representations with global relational reasoning at every level.

GNNs in visual perception. GNNs have been applied to scene graph generation, point-cloud processing, and scene understanding [8]. For 2D dense prediction,

a common strategy constructs a region adjacency graph from superpixels or detected objects and performs reasoning at the semantic level. In contrast, GraphDepth operates directly on convolutional feature maps, using pixel-level graph nodes, enabling end-to-end training without an intermediate segmentation step.

Uncertainty in depth estimation. Kendall and Gal [18] formalized aleatoric and epistemic uncertainty in Bayesian deep learning. Aleatoric uncertainty estimation—modelling observation noise as a learned per-pixel variance—has been applied to depth completion and stereo matching but remains under-explored in monocular depth architectures. We incorporate it both as an output head and as a weighting mechanism for the training loss.

3. Methodology

3.1. Overall Architecture

GraphDepth (Figure 1) is a four-stage encoder-bottleneck-decoder-output pipeline:

- 1. ResNet-101 Encoder.** Extracts multi-scale features $\{x_i\}_{i=1}^4$ at spatial resolutions 1/4, 1/8, 1/16, and 1/32 of the input.
- 2. Efficient GraphSAGE Modules.** Applied at the bottleneck (1/32) and the first two decoder stages (1/16, 1/8) for relational reasoning.
- 3. Attention-based Decoder.** Channel attention fuses skip connections with upsampled features at each decoder stage.
- 4. Multi-head Output.** Jointly predicts a dense depth map $D \in \mathbb{R}^{H \times W}$ and a pixel-wise uncertainty map $U \in \mathbb{R}^{H \times W}$.

3.2. Graph Construction

We treat each spatial location in a feature map as a graph node and define two complementary adjacency strategies.

Fixed Grid Graph. Each node connects to its 8-connected spatial neighbors:

$$A_{ij} = \begin{cases} 1 & \text{if } \|p_i - p_j\|_\infty \leq 1 \\ 0 & \text{otherwise} \end{cases} \quad (1)$$

where $p_i \in \mathbb{Z}^2$ is the pixel coordinate of node i . This strategy is computationally cheap and well-suited to scenes with predominantly local structure (e.g. indoor environments).

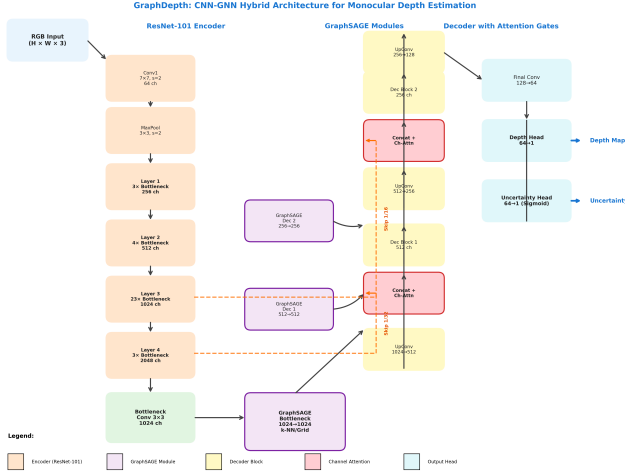


Figure 1: Overview of GraphDepth. GraphSAGE layers are embedded at multiple scales within the U-Net decoder, enabling hierarchical relational reasoning alongside local convolutional features.

Algorithm 1 Batch-Parallelized GraphSAGE

- 1: **procedure** BATCHGRAPHSAGE(X, H, W, B)
 - 2: $\triangleright X \in \mathbb{R}^{B \times C \times H \times W}$
 - 3: $X_{\text{flat}} \leftarrow \text{reshape}(X, (B \cdot H \cdot W, C))$
 - 4: $A \leftarrow \text{BuildGraph}(H, W)$ \triangleright Grid or k -NN
 - 5: $\mathbf{b} \leftarrow [0, \dots, 0, 1, \dots, 1, \dots, B-1]$ \triangleright batch vector
 - 6: $Y_{\text{flat}} \leftarrow \text{SAGEConv}(X_{\text{flat}}, A, \mathbf{b})$
 - 7: $Y \leftarrow \text{reshape}(Y_{\text{flat}}, (B, C, H, W))$
 - 8: **return** Y
 - 9: **end procedure**
-

Adaptive k -NN Graph. Edges are formed based on a combined feature-spatial distance:

$$d_{ij} = \alpha \|f_i - f_j\|_2 + \beta \|p_i - p_j\|_2 \quad (2)$$

where $f_i \in \mathbb{R}^C$ is the feature vector at node i , with $\alpha = 0.7$ and $\beta = 0.3$. Each node connects to its k nearest neighbors under d_{ij} . This data-dependent connectivity is better suited to aerial imagery, where semantically similar regions (terrain patches, roads) may be spatially distant.

3.3. Batch-Parallelized GraphSAGE Module

Naïve GNN implementations iterate over batch elements sequentially, imposing severe GPU underutilization. We avoid this via a *flat-batch* formulation that processes all images simultaneously by broadcasting a shared graph topology and using batch indices to partition the message-passing computation. The procedure is summarized in Algorithm 1.

The GraphSAGE update for node v at layer l is:

$$h_v^{(l+1)} = \sigma \left(W^{(l)} \cdot \text{CONCAT} \left(h_v^{(l)}, \frac{1}{|\mathcal{N}(v)|} \sum_{u \in \mathcal{N}(v)} h_u^{(l)} \right) \right) \quad (3)$$

where $\mathcal{N}(v)$ is the neighborhood of v , $W^{(l)}$ is a learnable weight matrix, and σ is the ReLU activation. Mean aggregation is chosen for its simplicity and stability; other aggregators (max, LSTM) were evaluated but yielded negligible gains.

3.4. Channel Attention for Skip Connections

Encoder skip connections carry both useful structural information and domain-specific noise. We apply a Squeeze-and-Excitation-style channel attention gate [16] before concatenation:

$$\text{CA}(X) = \sigma(W_2 \delta(W_1 \text{GAP}(X))) \odot X \quad (4)$$

where GAP is global average pooling, δ is ReLU, σ is sigmoid, and \odot is channel-wise multiplication. The reduction ratio is set to 16.

3.5. Loss Function

The total training loss combines an ℓ_1 reconstruction term, an image-gradient regularizer, and a heteroscedastic uncertainty term:

$$\mathcal{L}_{\text{total}} = \alpha \mathcal{L}_{\ell_1} + \beta \mathcal{L}_{\text{grad}} + \gamma \mathcal{L}_{\text{unc}} \quad (5)$$

$$\mathcal{L}_{\ell_1} = \frac{1}{N} \sum_{i=1}^N |y_i - \hat{y}_i| \quad (6)$$

$$\mathcal{L}_{\text{grad}} = \frac{1}{N} \sum_{i=1}^N (|\nabla_x y_i - \nabla_x \hat{y}_i| + |\nabla_y y_i - \nabla_y \hat{y}_i|) \quad (7)$$

$$\mathcal{L}_{\text{unc}} = \frac{1}{N} \sum_{i=1}^N \left(\frac{|y_i - \hat{y}_i|}{e^{s_i}} + s_i \right) \quad (8)$$

with $\alpha = 0.85$, $\beta = 0.15$, $\gamma = 0.50$, and $s_i = \log \hat{\sigma}_i^2$ the predicted log-variance at pixel i . The uncertainty term follows the formulation of Kendall and Gal [18]: the network is penalized less for errors where it is confident and more where it is overconfident.

3.6. Full Forward Pass

Algorithm 2 summarizes the complete inference pipeline.

Algorithm 2 GraphDepth Forward Pass

Require: RGB image $I \in \mathbb{R}^{3 \times H \times W}$ **Ensure:** Depth D , Uncertainty $U \in \mathbb{R}^{H \times W}$

```
1: ▷ Encoder
2:  $\{x_i\}_{i=1}^4 \leftarrow \text{ResNet101}(I)$ 
3: ▷ Bottleneck + GNN
4:  $b \leftarrow \text{GraphSAGE}(\text{Conv}_{3 \times 3}(x_4))$ 
5: ▷ Decoder
6:  $g_0 \leftarrow b$ 
7: for  $l \in \{1, 2, 3\}$  do
8:    $d_l \leftarrow \text{Upsample}(g_{l-1})$ 
9:    $s_l \leftarrow \text{CA}(\text{Concat}(d_l, x_{5-l}))$ 
10:  if  $l \leq 2$  then
11:     $g_l \leftarrow \text{GraphSAGE}(s_l)$ 
12:  else
13:     $g_l \leftarrow s_l$ 
14:  end if
15: end for
16: ▷ Heads
17:  $D \leftarrow \text{DepthHead}(g_3)$ 
18:  $U \leftarrow \text{UncertaintyHead}(g_3)$ 
19: return  $D, U$ 
```

4. Experiments

4.1. Datasets and Evaluation Protocol

We evaluate on four benchmarks spanning indoor, aerial, and synthetic domains (Table 1). **Mid-Air** is used exclusively for zero-shot testing (no fine-tuning) using the WHU-pretrained model, assessing cross-domain generalization to synthetic aerial data.

Table 1: Dataset characteristics and evaluation protocols.

Dataset	Type	Res.	Train	Test	Range	Metrics
NYU [10]	Indoor	640×480	50K	654	0.5–10m	δ_1 , RMSE
WHU [11]	Aerial	1024×1024	6,000	2,000	0–1,000m	RMSE, Rel
ETH3D [12]	Stereo	640×480	27	20	0–80m	Bad-2, MAE
Mid-Air [13]	Synth. aerial	1024×1024	–	4,200	0–1,000m	RMSE, δ_1

4.2. Implementation Details

Table 2: Implementation configurations per dataset.

Config	NYU / ETH3D	WHU	Mid-Air (test)
Input resolution	512×512	384×768	512×512
Optimizer	AdamW	AdamW	–
Learning rate	1×10^{-4}	5×10^{-5}	–
Batch size	8	4	–
Epochs	100	150	–
Precision	FP16 mixed	FP16 mixed	FP32
Graph type	Grid (8-conn)	k -NN ($k = 16$)	k -NN ($k = 16$)

All experiments use NVIDIA RTX 5070 Ti and A6000 GPUs. We apply gradient clipping (max norm 1.0) and a cosine annealing learning rate schedule. Aerial datasets use larger k -NN graphs ($k = 16$) to capture long-range terrain relationships absent in indoor scenes.

4.3. Main Results

4.3.1. In-Domain Performance

Table 3 compares GraphDepth against CNN and transformer baselines across all three in-domain benchmarks.

Key observations:

- **NYU Depth V2.** GraphDepth is within 4.6% of the best transformer (DepthFormer) on RMSE while running $2.9\times$ faster, demonstrating a favorable accuracy-efficiency trade-off.
- **WHU Aerial.** GraphDepth achieves the best result across all methods, with a 24.8% RMSE reduction over DepthFormer. We attribute this to the k -NN graph’s ability to connect semantically similar but spatially distant terrain regions.
- **ETH3D.** Strong second-best results on fronto-parallel stereo data confirm generalization beyond standard camera configurations.

4.3.2. Cross-Domain Generalization (Zero-Shot)

Table 4 evaluates models trained on WHU, transferred without adaptation to Mid-Air synthetic aerial imagery.

GraphDepth achieves a +10.3% improvement in δ_1 over DPT-Large. We attribute this to three complementary factors: (i) GraphSAGE’s explicit relational modeling generalizes across aerial viewpoints with varying altitude and terrain type; (ii) the uncertainty head suppresses overconfident predictions in out-of-distribution regions; and (iii) the k -NN graph topology adapts to varying terrain scales during inference without retraining.

4.4. Ablation Studies

4.4.1. Component Ablation on NYU Depth V2

Table 5 validates each architectural component.

Findings: (1) Each component contributes incrementally; the full model achieves a 7.2% RMSE reduction over the baseline. (2) Replacing GraphSAGE with a transformer yields a marginal 0.4% accuracy gain at the cost of 36% more FLOPs and $1.4\times$ slower inference—a poor trade-off. (3) The uncertainty head adds $< 1\%$ parameters but enables confidence-aware inference, especially beneficial under domain shift.

Table 3: Performance comparison across datasets. **Bold:** best result. Underlined: second best.

Method	NYU Depth V2			WHU Aerial			ETH3D		
	RMSE↓	Abs Rel↓	δ_1 ↑	RMSE↓	Rel↓	δ_1 ↑	Bad-2↓	MAE↓	Time (ms)
<i>CNN-based</i>									
U-Net [14]	0.563	0.123	0.845	15.32	0.184	0.712	8.42	0.89	24
ResNet-101 U-Net	0.541	0.118	0.858	14.18	0.172	0.738	7.95	0.82	31
BTS [4]	0.479	0.110	0.871	12.45	0.158	0.765	6.12	0.71	45
<i>Transformer-based</i>									
DPT-Large [6]	0.423	0.098	0.892	11.82	0.145	0.788	5.45	0.64	98
DepthFormer [7]	0.409	0.095	0.901	<u>10.95</u>	<u>0.138</u>	<u>0.802</u>	4.98	0.58	112
<i>GNN-based (ours)</i>									
GraphDepth	<u>0.428</u>	<u>0.102</u>	<u>0.885</u>	8.24	0.129	0.821	<u>5.12</u>	<u>0.61</u>	38

Table 4: Zero-shot generalization: WHU \rightarrow Mid-Air.

Method	RMSE↓	Rel↓	δ_1 ↑
U-Net [14]	28.45	0.312	0.542
ResNet-101 U-Net	26.18	0.287	0.578
DPT-Large [6]	22.94	0.245	0.645
GraphDepth (ours)	19.76	0.198	0.712

Table 5: Ablation study on NYU Depth V2 validation set.

Configuration	RMSE↓	Rel↓	δ_1 ↑	Params (M)	FLOPs (G)	FPS†
ResNet-101 U-Net (baseline)	0.541	0.118	0.858	54.2	128	31
+ GraphSAGE at bottleneck	0.528	0.114	0.867	56.8	135	29
+ Multi-scale GraphSAGE	0.515	0.111	0.875	58.1	142	27
+ Channel attention	0.509	0.109	0.879	58.1	142	26
+ Uncertainty head	0.506	0.108	0.882	58.3	143	25
+ Adaptive k -NN	0.502	0.107	0.885	58.3	145	25
Replace GNN with Transformer	0.498	0.106	0.887	62.5	198	18
Replace GNN with MLP-Mixer	0.518	0.112	0.872	59.1	156	22

4.4.2. Graph Topology Ablation

Table 6 examines the impact of graph connectivity across datasets.

Table 6: Graph configuration impact across datasets.

Graph Type	NYU		WHU		Mid-Air (0-shot)	
	RMSE	FPS	RMSE	FPS	RMSE	δ_1
Grid (4-conn)	0.512	28	11.45	32	21.23	0.685
Grid (8-conn)	0.508	26	11.02	30	20.45	0.698
k -NN ($k = 8$)	0.505	24	10.68	27	20.12	0.705
k -NN ($k = 16$)	0.502	22	10.24	24	19.76	0.712
k -NN ($k = 32$)	0.501	18	10.31	19	19.89	0.708

Grid graphs suffice for indoor scenes with predominantly local structure, while k -NN with $k = 16$ is optimal for aerial datasets. Increasing to $k = 32$ provides diminishing returns at significant throughput cost.

4.5. Computational Efficiency

Table 7 compares memory, parameters, and throughput.

Table 7: Computational efficiency comparison at 384×768 resolution.

Method	Params (M)	FLOPs (G)	Mem. (GB)	FPS†
DPT-Large [6]	310	478	10.2	10
DepthFormer [7]	280	412	8.8	9
BTS [4]	47	189	4.5	22
GraphDepth (ours)	58	145	3.8	25

Key advantages: (1) **Real-time capable**—25 FPS versus 9–10 FPS for transformers. (2) **Consumer GPU friendly**—3.8 GB VRAM fits on an RTX 3060. (3) **Scalable**—grid graphs support 1024×1024 inference at 12 FPS without architectural changes.

5. Limitations and Future Work

While GraphDepth demonstrates strong performance, we identify three areas for future development.

k -NN construction overhead. Adaptive graphs add 15–20% inference latency due to k -NN search. Approximate nearest-neighbor methods (e.g. LSH, FAISS) could reduce this to under 5%.

Sparse depth supervision. Our evaluation uses dense ground-truth depth maps. Extension to sparse LiDAR guidance—common in automotive settings—is ongoing and would require adapting the loss mask.

Temporal consistency. Single-frame processing ignores temporal coherence in video streams. Spatio-temporal graph construction connecting corresponding nodes across frames is a natural next step for video depth estimation.

6. Conclusion

We presented GraphDepth, an efficient hybrid CNN-GNN architecture for monocular depth estimation. By embedding batch-parallelized GraphSAGE layers at multiple scales of a ResNet-101 U-Net, we achieve explicit relational reasoning with linear computational complexity, combined with channel attention for adaptive skip-connection fusion and heteroscedastic uncertainty estimation for confidence-aware training. GraphDepth achieves state-of-the-art results on WHU Aerial, competitive performance on NYU Depth V2 and ETH3D, and superior zero-shot cross-domain transfer to Mid-Air—all at $2.6\times$ lower VRAM and $2.8\times$ higher throughput than leading transformer baselines. These results establish GNN integration as a principled and practically attractive alternative to attention for dense depth prediction.

References

- [1] D. Eigen, C. Puhrsch, and R. Fergus, “Depth map prediction from a single image using a multi-scale deep network,” *Advances in Neural Information Processing Systems (NeurIPS)*, 2014.
- [2] I. Laina, C. Rupprecht, V. Belagiannis, F. Tombari, and N. Navab, “Deeper depth prediction with fully convolutional residual networks,” *International Conference on 3D Vision (3DV)*, 2016.
- [3] H. Fu, M. Gong, C. Wang, K. Batmanghelich, and D. Tao, “Deep ordinal regression network for monocular depth estimation,” *IEEE/CVF CVPR*, 2018.
- [4] J. Lee, M. Han, D. Ko, and I. Suh, “From big to small: Multi-scale local planar guidance for monocular depth estimation,” *arXiv:1907.10326*, 2019.
- [5] S. Bhat, I. Alhashim, and P. Wonka, “AdaBins: Depth estimation using adaptive bins,” *IEEE/CVF CVPR*, 2021.
- [6] R. Ranftl, A. Bochkovskiy, and V. Koltun, “Vision transformers for dense prediction,” *IEEE/CVF ICCV*, 2021.
- [7] Z. Li, X. Wang, X. Liu, and J. Yang, “DepthFormer: Exploiting long-range correlation and local information for accurate monocular depth estimation,” *arXiv:2203.14211*, 2022.
- [8] Y. Li, G. Chen, X. Jin, Q. Wu, and Z. Cui, “Graph-based context reasoning for scene understanding,” *European Conference on Computer Vision (ECCV)*, 2020.
- [9] W. L. Hamilton, R. Ying, and J. Leskovec, “Inductive representation learning on large graphs,” *Advances in Neural Information Processing Systems (NeurIPS)*, 2017.
- [10] N. Silberman, D. Hoiem, P. Kohli, and R. Fergus, “Indoor segmentation and support inference from RGBD images,” *European Conference on Computer Vision (ECCV)*, 2012.
- [11] S. Ji, F. Wei, M. Lu, and L. Wang, “WHU: A large-scale dataset for stereo depth estimation in aerial scenarios,” *IEEE Transactions on Geoscience and Remote Sensing*, vol. 60, pp. 1–15, 2022.
- [12] T. Schöps *et al.*, “A multi-view stereo benchmark with high-resolution images and multi-camera videos,” *IEEE/CVF CVPR*, 2017.
- [13] M. Fonder, D. Defrance, and M. Van Droogenbroeck, “Mid-Air: A multi-modal dataset for extremely low altitude drone flights,” *IEEE/CVF CVPRW*, 2019.
- [14] O. Ronneberger, P. Fischer, and T. Brox, “U-Net: Convolutional networks for biomedical image segmentation,” *MICCAI*, 2015.
- [15] K. He, X. Zhang, S. Ren, and J. Sun, “Deep residual learning for image recognition,” *IEEE/CVF CVPR*, 2016.
- [16] J. Hu, L. Shen, and G. Sun, “Squeeze-and-excitation networks,” *IEEE/CVF CVPR*, 2018.
- [17] S. Woo, J. Park, J.-Y. Lee, and I. S. Kweon, “CBAM: Convolutional block attention module,” *European Conference on Computer Vision (ECCV)*, 2018.
- [18] A. Kendall and Y. Gal, “What uncertainties do we need in Bayesian deep learning for computer vision?” *Advances in Neural Information Processing Systems (NeurIPS)*, 2017.